Published in final edited form as:
Steroids. 2011 December 11; 76(13): 1465–1473. doi:10.1016/j.steroids.2011.07.017.

Phenylalanine 93 of the human UGT1A10 plays a major role in the interactions of the enzyme with estrogens

Camilla Höglund[1,a,b], **Nina Sneitz**[1,a,b], **Anna Radominska-Pandya**[c], **Liisa Laakonen**[a], and **Moshe Finel**[a]

[a]Centre for Drug Research, Faculty of Pharmacy, P.O. Box 56 (Viikinkaari 5), FI-00014 University of Helsinki, Finland [b]Division of Pharmaceutical Chemistry, Faculty of Pharmacy, P.O. Box 56 (Viikinkaari 5), FI-00014 University of Helsinki, Finland [c]Department of Biochemistry and Molecular Biology, University of Arkansas for Medical Sciences, Little Rock, Arkansas, USA (A.R.-P.)

Abstract

Little is currently known about the substrate binding site of the human UDP-glucuronosyltransferases (UGTs) and the structural elements that affect their complex substrate selectivity. In order to further understand and extend our earlier findings with phenylalanines 90 and 93 of UGT1A10, we have replaced each of them with Gly, Ala, Val, Leu, Ile or Tyr, and tested the activity of the resulting 12 mutants toward 8 different substrates. Apart from scopoletin glucuronidation, the F90 mutants other than F90L were nearly inactive, while the F93 mutants' activity was strongly substrate dependent. Hence, F93L displayed high entacapone and 1-naphthol glucuronidation rates, whereas F93G, which was nearly inactive in entacapone glucuronidation, was highly active toward estradiol, estriol and even ethinylestradiol, a synthetic estrogen that is a poor substrate for the wild-type UGT1A10. Kinetic analyses of 4-nitrophenol, estradiol and ethinylestradiol glucuronidation by the mutants that catalyzed the respective reactions at considerable rates, revealed increased K_m values for 4-nitrophenol and estradiol in all the mutants, whilst the K_m values of F93G and F93A for ethinylestradiol were lower than in control UGT1A10. Based on the activity results and a new molecular model of UGT1A10, it is suggested that both F90 and F93 are located in a surface helix at the far end of the substrate binding site. Nevertheless, only F93 directly affects the selectivity of UGT1A10 toward large and rigid estrogens, particularly those with substitutions at the D ring. The effects of F93 mutations on the glucuronidation of smaller or less rigid substrates are indirect, however.

1. Introduction

The UDP-glucuronosyltransferases (UGTs) are membrane bound enzymes of the endoplasmic reticulum that catalyze the conjugation of many compounds with glucuronic acid from UDP-glucuronic acid (UDPGA) (Wells et al., 2004). This glucuronidation reaction increases the water-solubility of mostly lipophilic substrates and stimulates their excretion from the body through bile or urine. The 19 functional human UGTs of subfamilies 1A, 2A and 2B (Mackenzie et al., 2005) are expressed in a tissue-specific manner. Many of them are expressed in the liver, but some are only or mainly expressed in

Corresponding author: Dr. Moshe Finel, Centre for Drug Research (CDR), Faculty of Pharmacy, P.O. Box 56 (Viikinkaari 5), FI-00014 University of Helsinki, Finland. moshe.finel@helsinki.fi, Fax: +358 9 1915 9556.
[1]These authors contributed equally to this study

extrahepatic tissues. UGT1A10, the subject of this study, belongs to the latter group and it is mainly expressed in the intestine (Ohno and Nakajin, 2009; Itäaho et al., 2009).

Most human UGTs can catalyze the glucuronidation of several compounds that vary greatly in structure, size and physicochemical properties. This promiscuity leads to partial overlaps in the substrate selectivity of individual UGTs, although closer inspection of their kinetic properties, as well as regio- and stereo-selectivity, reveals that there are clear differences even among highly homologous individual UGTs such as 1A7-1A10 (Fujiwara et al., 2009; Itäaho et al., 2010). The crystal structure of C-domain of UGT2B7, the domain that contains the UDPGA (co-substrate) binding site, has been resolved (Miley et al., 2007), but it does not include the binding site for the aglycone substrate. Based on the homology between UGTs and other glycosyltransferases, UGTs are predicted to be comprised of two large pseudosymmetric α-β sandwich domains, the N and C domains, and two additional small domains, the envelope helices connecting the globular domains, and a transmembrane helix with a short cytoplasmic tail (Laakkonen and Finel, 2010). In mature UGT1A10, the N-terminal domain, the C-terminal domain, the envelope helices and the transmembrane domain are predicted to correspond to residues 26–277, 278–430, 431–468 and 469–530, respectively. In analogy to resolved crystal structures of homologous glycosyltransferases from plant and bacteria, UDPGA very likely binds to the cleft between the N and the C domains, and is stabilized by several conserved, specific interactions to the C domain. In UGT1A10, UDPGA is probably bound by C-domain residues between W351 to Q394, and at the same time situated close to His37 of the N-terminal domain, the “catalytic His”, that directly contributes to *O*-glucuronidation reactions by stabilizing the deprotonated form of the hydroxyl group on the substrate (Miley et al., 2007; Patana et al., 2007 and 2008). Contrary to the binding site of UDPGA, the exact location and architecture of the acceptor-substrate binding site is currently unknown. The available data suggests that two variable segments in the N-domain, L83-H123 and I172-F224 (UGT1A10 numbering), contribute to the substrate binding site. We hypothesize that the actual interaction residues will vary from case to case, even if provided by these segments. The complex substrate selectivity of the UGTs -promiscuous and specific at the same time - suggests that part of the binding site is rigidly refined and part is flexible. The latter process may be affected by the substrate itself in an induced fit manner.

UGT1A10 is highly active in the glucuronidation of estrogens and several other compounds (Xiong et al., 2006; Starlard-Davenport et al., 2007; Dellinger et al., 2007; Zielinska et al., 2008; Itäaho et al., 2008 and 2010). A photoaffinity labeling study, using 4-azido-2-hydroxybenzoic acid as a probe, suggested that F90 and F93 of UGT1A10 are important for interaction with phenolic substrates (Xiong et al., 2006). We have now undertaken to explore this site in more detail, using site directed mutagenesis, activity analyses of steroids, coumarins and aromatic alcohols, and homology modeling. The results shed new light on glucuronidation of several substrates by UGT1A10, as well as raise many new questions.

2. Materials and Methods

Materials, recombinant UGT1A10, and mutants

Scopoletin, 1-naphthol, 17β-estradiol, 4-nitrophenol (pNP), 16α,17β-estriol, ethinylestradiol (EED), 4-methylumbelliferone, (4-MU), UDPGA (triammonium salt) and D-saccharic acid 1,4-lactone were purchased from Sigma-Aldrich (St. Louis, MO, USA). Sodium dihydrogen phosphate dihydrate was from Fluka (Buchs, Switzerland) and perchloric acid was from Merck (Darmstadt, Germany). Entacapone was a generous gift from Orion Pharma (Espoo, Finland).

The mutations in F90 and F93 of UGT1A10 were generated by the QuikChange system (Stratagene, La Jolla, CA, USA) and the sequence of the entire cloned UGT1A10 was verified by DNA sequencing. Recombinant human UGT1A10 and the mutants were expressed as His-tagged proteins in baculovirus-infected Sf9 insect cells as previously described (Kurkela et al., 2003; Kuuranne et al., 2003). The relative expression level of the UGT in each membrane batch was determined using the monoclonal anti-His antibodies tetra-His (Qiagen, Hilden, Germany) as detailed elsewhere (Kurkela et al., 2007). The expression level of the variant with the lowest expression per mg protein, F90L, was taken as the reference whose expression level is 1.0. The corresponding levels of the other samples were: UGT1A10, 2.0; F90A, 7.3; F90G, 6.4; F90V, 11.5; F90I, 7.8; F90Y, 1.4; F93A, 7.6; F93L, 4.3; F93G, 5.6; F93V, 10.2; F93I, 10.8; F93Y, 2.6. Protein concentrations were determined by the BCA method (Pierce Biotechnology, Rockford, IL, USA).

Glucuronidation activity analyses

Glucuronidation rates at a single protein and substrate concentrations (“screening assays”) were measured in duplicates (at most 15% difference between duplicates), in a final volume of 100 µl. In addition, the kinetics of pNP, estradiol and EED were determined, and in these assays triplicates were used. The protein concentrations for the screenings and the kinetics were 20–200 µg/ml, depending on the tested substrate and enzyme variant. The screening reaction mixtures contained 50 mM phosphate buffer, pH 7.4, 5 mM $MgCl_2$, 5 mM saccharolactone, 5 mM UDPGA and the following concentrations of the tested substrates: 500 µM in the cases of scopoletin, pNP, entacapone and estriol, 200 µM of 4-MU, or 100 µM for the screening assays with estradiol, EED and 1-naphthol. Estradiol, EED and estriol were dissolved in DMSO and the final concentration of the solvent in assays with these substrates was either 5% (estradiol and estriol), or 10% (EED). These concentrations of DMSO do not inhibit the activity of recombinant UGTs (Zhang et al., 2011).

Saccharolactone was included in the first screening analyses, but once it became clear that this inhibitor of beta glucuronidase activity does not improve the activity results (Oleson and Court, 2008), it was left out of subsequent assays. Hence, the estradiol and EED screenings and all the kinetic analyses were carried out in the absence of saccharolactone. The reactions were started by the addition of UDPGA, followed by mixing and transfer to 37°C. The reactions were carried out for 60 min in the cases of pNP and EED, 30 min for estradiol, estriol, 4MU, 1-naphthol and entacapone, or 20 min in the case of scopoletin. The incubations were terminated by adding 10 µl perchloric acid, cooling on ice for 10 min, and subsequent centrifugation at 16000 *g* for 10 min. The supernatants from the latter centrifugation were subjected to HPLC analysis.

The HPLC analyses were carried out on either an Agilent (1100 series, Agilent Technologies, Palo Alto, CA, USA), or a Shimadzu HPLC (LC-10 model, Shimadzu Corporation, Kyoto, Japan). These two HPLCs were equipped with both UV absorbance and fluorescence detectors. The estradiol-3-glucuronide was separated from the estradiol 17-glucuronide using Chromolith SpeedRod column (Merck, Darmstadt, Germany). The column temperature was 30°C. The mobile phase consisted of 60% 25 mM phosphate buffer, pH 3, and 40% methanol. The flow rates were as follow: 0 – 9.5 min, 1 ml/min; 9.5 – 19 min, 2 ml/min; 19 – 20 min, 1 ml/min. The glucuronides were detected by fluorescence (excitation 216 nm, emission 316 nm) and the retention time for estradiol-3-glucuronide was 5.0 min. Estriol and its 3-glucuronide were separated using Hypersil BDS-C18, 5µm, 4,6 × 150mm (Agilent Technologies, Palo Alto, CA) and recorded with fluorescence detection (excitation 280 nm, emission 305 nm). The column temperature was 40°C. The mobile phase consisted of 65% 25 mM phosphate buffer, pH 3 and 35% methanol and the flow rate was 1 ml/min. The retention time for estriol-3- glucuronide was 3.8 min. The HPLC analyses for scopoletin, 1-naphthol, 4-nitrophenol, entacapone and 4-methylumbelliferone

were performed as previously described (Kurkela et al., 2004; Luukkanen et al., 2005). The EED glucuronide was detected as described (Luukkanen et al., 2005), but using the Shimadzu HPLC.

Glucuronides of scopoletin and EED were quantified using [^{14}C]-UDPGA (Kaivosaari et al., 2001), whereas pNP, 1-naphthol, 4-MU, entacapone, estradiol-3-glucuronide and estriol-3-glucuronide were quantified using authentic standards (Luukkanen et al., 2005). The detection and quantification limits, respectively, were 0.8 and 2.5 μM for estradiol, 0.3 and 1.0 μM for estriol, 0.3 and 0.9 μM for EED, 1.1 and 3.6 μM for pNP, 2.1 and 7.0 μM for 4-MU, 0.02 and 0.06 μM for scopoletin, 0.03 and 0.1 μM for 1-naphthol and 0.6 and 1.9 μM for entacapone.

Kinetic analyses

Enzyme kinetics experiments were performed in triplicates. The assay conditions and reaction terminations were similar to the screening assays, but the protein concentrations and incubation times for these assays were selected according to the preliminary experiments in order to ensure that product formation was within the linear range with respect to both protein concentration and time, and that the substrate consumptions was less than 10%.

Kinetic constants were estimated by fitting the experimental data using GraphPad Prism for Windows (GraphPad Software, San Diego, CA, USA). In this study the data was fitted to either the Michaelis-Menten or the Michaelis-Menten with substrate inhibition models. The goodness of the fit, as calculated by the GraphPad Prism program, is indicated alongside the results in Table 1.

Modeling

The amino acid sequence of the mature human UGT1A10 (P22309 from the SwissProt database) (http://www.uniprot.org) was aligned to plant and bacterial glycosyltransferases of known structure, as described earlier (Laakkonen and Finel, 2010). The sequence-to-structure match was modified from the published alignment so that the short helices observed in 2D0Q and 2IYA were used as templates for the first predicted helix in loop 3. A homology model was constructed for the mature human UGT1A10 from the structural alignment with the program Modeller 9v6, similarly to the work with UGT1A1 (Laakkonen and Finel, 2010). The model includes UDPGA.

The substrate structures were built and optimized in MOPAC2009 (http://openmopac.net) with PM3 methodology (Stewart, 2007), and docked into the active site guided by the interactions with the reactive site histidine (His37) and the UDPGA. The same nomenclature for the secondary structure elements was used as before: the core strands of the globular domains are numbered sequentially, and named by the domain, e.g. Nβ1. The following helix bears the same name, e.g. Nα1, followed by additional numbers when the inter-strand segment contains more than one helix, e.g. Nα3-1. Amino acid numbers refer to the nascent full length UGT1A10.

3. Results

We have previously identified F90 and F93 of the human UGT1A10 as residues that form covalent bonds with 4-azido-2-hydroxybenzoic acid upon photolabeling (Xiong et al., 2006). Replacing these two phenylalanine residues with either Ala or Leu was then shown to reduce glucuronidation activity toward 4-nitrophenol (pNP) and 4-methylumbelliferone (4-MU) (Xiong et al., 2006), and to variably affect the glucuronidation of native and hydroxylated estrogens (Starlard-Davenport et al., 2007). This suggested that F90 and F93 may form part of the substrate binding site of UGT1A10 and in order to gain further insight

into the active site properties, we have now examined the effect of other amino acids at the same positions. Both these Phe residues were separately replaced with 6 different residues, either the aromatic Tyr, or amino acids with increasing side chain size and hydrophobicity, namely Gly, Ala, Leu, Val and Ile. The 12 resulting single mutants were expressed in baculovirus-infected insect cells and their activities, corrected for relative expression level, were compared to wild type UGT1A10. The aglycone substrates in this study included the simple aromatics pNP and 1-naphthol, the coumarins scopoletin and 4-MU, the estrogens estradiol, estriol and EED, and a less commonly tested drug, entacapone, an inhibitor of catechol O-methyltransferase (COMT) and a very good substrate of UGT1A9 (Lautala et al., 2000) (Fig. 1).

Activity screens

The mutant enzymes were initially studied for glucuronidation activity toward a panel of substrates. In these screens a single and relatively high substrate concentration was used and protein concentration for the screening experiments of the different UGT1A10 variants was not optimized for each assay. Nevertheless, in no case more than 10% of the substrate was consumed during the reaction. The protein concentrations in these assays were mainly similar for all mutants and the glucuronidation rates were, subsequently, corrected (normalized) according to the relative expression level of the individual enzyme (see Methods). It may be added here that the differences in relative expression levels in the baculovirus-infected insect cells system that was used to produce the recombinant UGTs should not be taken as evidence for the effect of the mutation on the gene transcription, translation nor folding in the human intestine, would such mutations occur.

All the mutant enzymes exhibited activity at least towards scopoletin, suggesting that in each of them the protein is (largely) folded and that no elements essential for catalysis, such as UDPGA binding, were lost by the mutations. In addition, the results indicate that some degree of activity from barely detectable to high rates, was exhibited towards the small substrates by all enzyme variants, with the exception of 4-MU by F90Y. On the other hand, several or even the majority of mutants were unable to glucuronidate the larger substrates (Fig. 2).

pNP

Glucuronidation screen with pNP as the aglycone substrate revealed sharp differences between mutations at F90 to the corresponding mutations in F93. All the 6 mutations we have generated at the F90 position severely reduced the pNP glucuronidation rate, to 1 – 15% of wild type activity, whereas replacements of F93 with the same set of residues did not affect activity that much in most cases, yielding 10 – 85% of the wild type glucuronidation rate (Table 1 and Fig. 2). Interestingly, the leucine mutants at both positions, F90L and F93L, were least affected. Mutant F93G also exhibited considerable activity, about 60% of control.

It may be noted here that the screening assays were done prior to kinetic analyses with the selected mutants. As became clear to us later, and will become clear to the reader below, the calculated V_{max} values for some of the mutants were, eventually, higher than for UGT1A10, even if these mutants exhibited lower glucuronidation rates in the screening assays (Table 1). This was mainly due to a large increase in the apparent K_m value of these mutants, an important and interesting effect of the respective mutations that was only appreciated during the subsequent kinetic analyses (see below).

1-naphthol

The glucuronidation of 1-naphthol was least affected by the mutations, particularly those in F93. Similarly to the results with pNP, the leucine mutations at both positions were the most active in comparison to the corresponding mutations, respectively: F90L exhibited wild type rate, while F93L catalyzed 1-naphthol glucuronidation at about twice the rate of the control UGT1A10. Changing F93 to either G or Y did not affect the 1-naphthol glucuronidation rate, while the activity of F93I was about half the control rate. The F to V replacements in both positions yielded about one third of the control rate and the least active mutant was F90G (Fig. 2).

4-MU

The glucuronidation of 4-MU turned out to be highly sensitive to the mutations we have prepared. None of the 12 mutants exhibited similar, let alone higher 4-MU glucuronidation rate than the wild type (Fig. 2). The F to L replacements at both the F90 and F93 positions were the most active mutants in this case, exhibiting about a third of the control 4-MU glucuronidation rate. Mutants F90L, F93L and F93Y exhibited low but still significant activity, while the other mutants showed 10% or less of the control 4-MU glucuronidation rate. No activity toward 4-MU by the F90Y mutant was detected (Fig. 2). It may be added here that 4-MU glucuronidation was already examined in the first work about the F90A and F93A mutants (Xiong et al., 2006) and the results of the present study, that were obtained from separate assays in another laboratory, agree with the earlier results for these mutants.

Scopoletin

The activity of the tested enzymes toward scopoletin was radically different from that toward 4-MU, regardless the structural similarity of the two compounds. The scopoletin glucuronidation rates of the majority of the mutants were higher than control, up to six fold the (normalized) rate of UGT1A10 (Fig. 2). The two leucine mutants, F90L and F93L, were the most active ones; whereas the corresponding F to Y mutants were the only ones exhibiting scopoletin glucuronidation rates that were lower than control UGT1A10 (Fig. 2).

Entacapone

The drug entacapone is a UGT1A9-specific substrate when human liver microsomes are analyzed, but it is also glucuronidated by the (largely) extra-hepatic UGTs 1A7, 1A8 and 1A10 (Luukkanen et al., 2005). As a molecule, entacapone differs significantly from the other substrates that were selected for this study since it is rather large, very flexible and contains two strongly polar groups, a cyano and a nitro groups (Fig. 1). The screening results for entacapone glucuronidation rates show high variability: in 6 mutants the rates were very low, or below detection limit, while in F93L the rate was 2.5 fold higher than in control UGT1A10 (Fig. 2).

Estradiol

This estrogen has two hydroxyl groups, 3-OH and 17-OH, both of which can be glucuronidated. However, since UGT1A10 generates estradiol-3-glucuronide at nearly 100 fold higher rate than estradiol-17-glucuronide (Itäaho et al., 2008), we have concentrated in this study on the formation of estradiol-3-glucuronide. The results show that only 4 of the 12 mutants exhibited considerable estradiol glucuronidation rate. Two of them, F93G and F93Y, catalyzed estradiol glucuronidation at similar rates to control 1A10, while F90L and F93A exhibited about a quarter of the control rates (Fig. 2). The latter findings are in agreement with the results in a previous study that examined the estrogens glucuronidation activity of the F90L and F93A mutants of UGT1A10, along with several other UGTs (Starlard-Davenport et al., 2007).

Estriol

All the F90 and 4 out of the 6 F93 mutants were practically devoid of estriol glucuronidation activity. The only two mutants that exhibited considerable activity toward this estrogen were F93A and, notably, F93G. The activity of F93A in the estriol glucuronidation screen was about 60% of the control activity, whereas F93G, the mutant with the smallest side chain, catalyzed estriol glucuronidation at about 3 times higher rate than control UGT1A10 (Fig. 2).

Ethinylestradiol

Ethinylestradiol is generally regarded as a specific substrate for UGT1A1, at least when human liver microsomes are assayed (Soars et al., 2003). Nevertheless, we have noticed that UGT1A10, too, can catalyze EED glucuronidation at low rates, and included this aglycone substrate in the current study. The results of the EED glucuronidation screen revealed low but detectable activity by UG1A10, somewhat higher in the F93A mutant and, strikingly, very high activity toward this synthetic steroid by F93G, at least in comparison to UGT1A10 (Fig. 2).

Kinetic analyses

As useful as the screening results are for gaining an overall view of the effects of different mutations, much more detailed data about the interplay between enzyme and substrate can be gained from kinetics studies. To keep this study within manageable size, full kinetic assays were carried out with 3 of the substrates, pNP, estradiol and EED. The mutant enzymes that exhibited significant and easily detectable activity toward these compounds were included in these assays and the results are presented in Figure 3. The reactions generally followed either Michaelis-Menten or Michaelis-Menten with substrate inhibition kinetics. The derived kinetic constants, K_m, K_i and V_{max} (expression-normalized), are listed in Table 1. As can be seen from the results, in the cases of pNP and estradiol, the K_m values of the tested mutants were mostly higher than the corresponding values in UGT1A10. Interestingly, in the two mutants that catalyzed considerable rates of EED glucuronidation, the ratio of kinetic constant values between mutants and control were different. Mutant F93G exhibited lower K_m and much higher V_{max} values than UGT1A10, while in F93A both K_m and V_{max} values were lower than in the control (Table 1 and Fig. 3). The kinetic analyses of the EED glucuronidation reactions also indicated minor substrate inhibition in both F93G and F93A.

Homology model

In order to interpret the large amount of results we have generated in this study, it is important to locate F90 and F93 with respect to the catalytic centre of the enzyme, His37 and the bound UDPGA. To this end, we have modeled the protein similarly to our recent work with UGT1A1 (Laakkonen and Finel, 2010). The model indicates that phenylalanines 90 and 93 are located 15 and 18 residues, respectively, after Nβ1 (C72-K75), in a segment that is strongly predicted to be helical (Nα3-1) by both the PredictProtein and Jpred programs (Rost et al., 2004; Cole et al., 2008; respectively). This early part of loop 3 shows major structural variability and mobility among the resolved structures of glycosyltransferases from plant and bacteria, while the surrounding areas of the proteins overlap well (Fig. 4). Interestingly, this is a rather variable segment among the human UGTs, too. The two phenylalanines are conserved in the highly homologous UGTs 1A7–1A10 (Fig. 4), but not in many other UGTs. At position 90, F, Y, I, L, V and T are observed in other UGTs, while at position 93 the other UGTs carry either F, Y, H, I, L, M or Q. Notably, neither A nor G, and not any charged residues, are found in any of the sequences at the homologous positions (Fig. 4).

The predicted helix Nα3-1 is amphipathic. The derived model of the substrate binding site is shown with pNP and estradiol docked to the reactive center (Fig. 5). Both substrates are aromatic, rigid and planar, but differ largely in size. The much smaller pNP does not reach up to the studied phenylalanines, while the twice larger estradiol does. In the vicinity of the reactive center, however, the substrates occupy the same space. It may also be noted here that both phenylalanines are free to adopt several rotamers.

4. Discussion

Little is currently known about the aglycone substrate binding site, or sites, of individual UGTs and about the effects of different amino acids on the complex substrate selectivity of these enzymes. To address these issues we have explored the role(s) of F90 and F93 of UGT1A10, two residues that were previously reported to react with photoactive phenolic probes (Xiong et al., 2006). We have replaced these phenylalanine residues with either the aromatic tyrosine (least different), or with hydrophobic residues of increasing size, glycine, alanine, valine, leucine and isoleucine. In addition, we have selected several different substrates for this study, large and small (Fig. 1), in order to obtain a better view of the substrate selectivity of the different mutants. The substrates are all formally neutral, although they included compounds with the strongly polar nitro and cyano groups.

The high variability in the effects of different mutations, particularly at position 93 (Fig. 2), and the apparent dependence of these effects on the tested substrates, appears at first sight to be nearly impossible to understand. However, closer looks at the size and flexibility of the different substrates (Fig. 1), as well as the new model for the active site of UGT1A10 (Fig. 5), provide interesting insights and likely explanations for part of the findings.

As seen in the structures of homologous proteins, the active sites of the UGTs, and other glycosyltransferases related to them, lie in the cleft between the N and C domains (Osmani et al., 2009). The binding pocket is closed at one side by Nα1, and the substrates in the resolved structures have only limited positional freedom. The crystal structures show fully buried substrate analogs bound to the active site (Brazier-Hicks et al., 2007), suggesting that for a substrate molecule to enter and product to leave, the surface loops must rearrange. The surface loops of the N domain are very likely critical for the specificity differences between the human UGTs, as all the UGT1A enzymes are identical from E286 onward. A static model like ours cannot represent the whole sequence of events, but as no details on the activation mechanism of the UGTs are known, we consider the model an acceptable starting point.

The substrates used in this study can be divided, according to their size, into two groups. The small substrates group includes pNP, 1-naphthol, 4-MU, and scopoletin, whereas the large ones are entacapone and the three estrogens (Fig. 1). The effect of the size difference on the results can be addressed by placing the reactive hydroxyl groups of each substrate between the active site histidine, H37, and the bound UDPGA, while the rest of the substrate molecule is directed toward phenylalanines 90 and 93. In such an orientation, only the large substrates, represented in Fig. 5 by estradiol, but not the small substrates like pNP, reach to the segment containing these two Phe residues (Fig. 5).

The three estrogens differ from each other in ring D substitutions (Fig. 1) and among them the trend in the glucuronidation rates could be explained in the following way. Estradiol is glucuronidated effectively by UGT1A10, and two of the mutants at F93, F93G and F93Y, exhibit as high as control activity toward it (Fig 2). The glucuronidation activity of UGT1A10 and, particularly F93Y, decreases sharply with additional substituents on the steroid, either the hydroxyl at C16 in the case of estriol, or the ethinyl group at C17 of EED.

However, replacing phenylalanine at position 93 of UGT1A10 with the smallest side-chain amino acid, glycine, results in higher or even much higher glucuronidation rates of estriol and EED, respectively, in comparison to control UGT1A10 (Fig. 2). It is thus suggested that in the enzyme-substrate complex, the estradiol substituents on ring D of the steroid backbone occupy the same space as residue 93 of the protein. The outcome of this is that increasing the substrate size in this part of the binding site can be partly compensated by reducing the size of the side chain at position 93, as seen in estriol glucuronidation by mutant F93A and the glucuronidation of both estriol and EED by the F93G mutant (Fig. 2).

It may be added here that the F90 mutants, even F90L that exhibited about 25% of the control rate in estradiol glucuronidation, are nearly inactive toward estriol and EED (Fig. 2).

Scopoletin has an extended substitutent on the naphthol backbone, the methoxy group at a beta position with respect to the reactive hydroxyl (Fig. 1). The activity results of the mutants with scopoletin are a clear exception (Figs. 1 and 2) that we currently cannot explain. Nevertheless, it may be suggested that a combination of structural and physico-chemical properties makes the glucuronidation of scopoletin less dependent on interactions with other residues than the catalytic His and the bound UDPGA. In this respect, it may be noted here that addition of 0.2 % of the detergent Triton X-100 to the full-length membrane-bound UGT1A9, or the preparation of a water-soluble mutant of UGT1A9 by truncating the enzyme before the predicted start of the trans-membrane helix and the cytoplasmic tail affected the scopoletin glucuronidation activity of the enzyme differently than glucuronidation of other aglycone substrates (Kurkela et al., 2003 and 2004, respectively). It is thus assumed that the differences in glucuronidation rates of the F90 and F93 mutants toward scopoletin on one hand, and toward 4-MU on the other hand (Fig. 2) are linked in some way to the previous observations with UGT1A9 and these substrates (Kurkela et al., 2003 and 2004). Nevertheless, it remains to be studied how these findings are connected.

The homology model provides an explanation for the effects of the mutations on the activity of UGT1A10 toward the large substrates. It does not, however, yield a clear explanation for the variable results with the smaller substrates, such as pNP, 4-MU and 1-naphthol. Another observation that is not currently explained by the model is the differences between F90 and F93, and the much higher sensitivity of UGT1A10 to the replacement of F90 by other residues, except leucine (Fig. 2). The main current limitation in building a detailed model for the active site of the UGTs concerns the loops at the back of the substrate binding pocket. This is because the homologous glycosyltransferases from plant and bacteria for whom a solved structure is available (as a template for the modeling) mostly lack these loops (Fig. 4). In any case, these loops are predicted to be mobile and flexible to some extent, and they may be affected by the binding of UDPGA in an “induced fit” type of movement.

The results have shown that different replacements at positions 90 and 93 of UGT1A10 affect activity and kinetics in different ways. The results and the model are in agreement with the original suggestion that these residues are involved in substrate binding by UGT1A10 (not merely phenolic substrates, though) (Xiong et al., 2006). Nevertheless, it is most likely that these two phenylalanines are not the only major player in estrogens glucuronidation by UGT1A10. If they were, the highly homologous enzyme, UGT1A9, that has both Phe residues, should have also exhibited high glucuronidation rates toward the 3-OH of estradiol, but it is practically inactive with estradiol (Itäaho et al., 2008). Still, the latter study suggested that UGT1A9 binds estradiol since it inhibited the scopoletin glucuronidation activity of the enzyme (Itäaho et al., 2008), leaving open the possibility that either or both these phenylalanines play a role in estrogens binding to UGT1A9, too.

In summary, the results of this study suggest that F93 of the human UGT1A10 is involved in substrate binding, whereas the role of F90 is somewhat different. The new detailed structural model for this enzyme, as well as the wealth of activity results, are likely to stimulate new studies that will take us closer to understanding the complex substrate selectivity of the human UGTs, and the different steps in their catalytic cycle.

Abbreviations

4-MU	4-methylumbelliferone
pNP	4-nitrophenol
EED	ethinylestradiol
UDPGA	UDP-glucuronic acid
UGT	UDP-glucuronosyltransferase

Acknowledgments

We would like to thank Johanna Mosorin, Kaisa Laajanen and Johanna Troberg for skilful technical assistance at different stages of this study, and Orion Pharma Ltd. for providing entacapone.

Financial support: this study was supported, in parts, by the Sigrid Juselius Foundation (MF), the Magnus Ehrnrooth foundation (NS and LL), and by the NIH Grant GM075893 (AR-P).

References

Brazier-Hicks M, Offen WA, Gershater MC, Revett TJ, Lim EK, Bowles DJ, Davies GJ, Edwards R. Characterization and engineering of the bifunctional N- and O-glucosyltransferase involved in xenobiotic metabolism in plants. Proc Natl Acad Sci USA. 2007; 104:20238–20243. [PubMed: 18077347]

Cole C, Barber JD, Barton GJ. The Jpred 3 secondary structure prediction server. Nucleic Acids Res. 2008; 36(Web Server issue):W197–W201. [PubMed: 18463136]

Dellinger RW, Chen G, Blevins-Primeau AS, Krzeminski J, Amin S, Lazarus P. Glucuronidation of PhIP and N-OH-PhIP by UDP-glucuronosyltransferase 1A10. Carcinogenesis. 2007; 28:2412–2418. [PubMed: 17638922]

Fujiwara R, Nakajima M, Yamanaka H, Yokoi T. Key amino acid residues responsible for the differences in substrate specificity of human UDP-glucuronosyltransferase (UGT)1A9 and UGT1A8. Drug Metab Dispos. 2008; 37:41–46. [PubMed: 18832479]

Itäaho K, Mackenzie PI, Ikushiro S, Miners JO, Finel M. The configuration of the 17-hydroxy group variably influences the glucuronidation of beta-estradiol and epiestradiol by human UDP-glucuronosyltransferases. Drug Metab Dispos. 2008; 36:2307–2315. [PubMed: 18719240]

Itäaho K, Court MH, Uutela P, Kostiainen R, Radominska-Pandya A, Finel M. Dopamine is a low-affinity and high-specificity substrate for the human UDP-glucuronosyltransferase 1A10. Drug Metab Dispos. 2010a; 37:768–775.

Itäaho K, Laakkonen L, Finel M. How many and which amino acids are responsible for the large activity differences between the highly homologous UDP-glucuronosyltransferases (UGT) 1A9 and UGT1A10? Drug Metab Dispos. 2010b; 38:687–696.

Kaivosaari S, Salonen JS, Mortensen J, Taskinen J. High-performance liquid chromatographic method combining radiochemical and ultraviolet detection for determination of low activities of uridine 5'-diphosphate-glucuronosyltransferase. Anal Biochem. 2001; 292:178–187. [PubMed: 11355849]

Kurkela M, Garcia-Horsman JA, Luukkanen L, Morsky S, Taskinen J, Baumann M, Kostiainen R, Hirvonen J, Finel M. Expression and characterization of recombinant human UDP-glucuronosyltransferases (UGTs). UGT1A9 is more resistant to detergent inhibition than other UGTs and was purified as an active dimeric enzyme. J Biol Chem. 2003; 278:3536–3544. [PubMed: 12435745]

Kurkela M, Hirvonen J, Kostiainen R, Finel M. The interactions between the N-terminal and C-terminal domains of the human UDP-glucuronosyltransferases are partly isoform-specific, and may involve both monomers. Biochem Pharmacol. 2004; 68:2443–2450. [PubMed: 15548391]

Kurkela M, Patana AS, Mackenzie PI, Court MH, Tate CG, Hirvonen J, Goldman A, Finel M. Interactions with other human UDP-glucuronosyltransferases attenuate the consequences of the Y485D mutation on the activity and substrate affinity of UGT1A6. Pharmacogenet Genomics. 2007; 17:115–126. [PubMed: 17301691]

Kuuranne T, Kurkela M, Thevis M, Schanzer W, Finel M, Kostiainen R. Glucuronidation of anabolic androgenic steroids by recombinant human UDP-glucuronosyltransferases. Drug Metab Dispos. 2003; 31:1117–1124. [PubMed: 12920167]

Laakkonen L, Finel M. A molecular model of the human UDP-glucuronosyltransferase 1A1, its membrane orientation, and the interactions between different parts of the enzyme. Mol Pharmacol. 2010; 77:931–939. [PubMed: 20215562]

Lautala P, Ethell BT, Taskinen J, Burchell B. The specificity of glucuronidation of entacapone and tolcapone by recombinant human UDP-glucuronosyltransferases. Drug Metab Dispos. 2000; 28:1385–1389. [PubMed: 11038168]

Luukkanen L, Taskinen J, Kurkela M, Kostiainen R, Hirvonen J, Finel M. Kinetic characterization of the 1A subfamily of recombinant human UDP-glucuronosyltransferases. Drug Metab Dispos. 2005; 33:1017–1026. [PubMed: 15802387]

Mackenzie PI, Bock KW, Burchell B, Guillemette C, Ikushiro S, Iyanagi T, Miners JO, Owens IS, Nebert DW. Nomenclature update for the mammalian UDP glycosyltransferase (UGT) gene superfamily. Pharmacogenet Genomics. 2005; 15:677–685. [PubMed: 16141793]

Miley MJ, Zielinska AK, Keenan JE, Bratton SM, Radominska-Pandya A, Redinbo MR. Crystal structure of the cofactor-binding domain of the human phase II drug-metabolism enzyme UDP-glucuronosyltransferase 2B7. J Mol Biol. 2007; 369:498–511. [PubMed: 17442341]

Ohno S, Nakajin S. Determination of mRNA expression of human UDP-glucuronosyltransferases and application for localization in various human tissues by real-time reverse transcriptase-polymerase chain reaction. Drug Metab Dispos. 2009; 37:32–40. [PubMed: 18838504]

Oleson L, Court MH. Effect of the beta-glucuronidase inhibitor saccharolactone on glucuronidation by human tissue microsomes and recombinant UDP-glucuronosyltransferases. J Pharm Pharmacol. 2008; 60:1175–1182. [PubMed: 18718121]

Osmani SA, Bak S, Møller BL. Substrate specificity of plant UDP-dependent glycosyltransferases predicted from crystal structures and homology modeling. Phytochemistry. 2009; 70:325–347. [PubMed: 19217634]

Patana AS, Kurkela M, Goldman A, Finel M. The human UDP-glucuronosyltransferase: identification of key residues within the nucleotide-sugar binding site. Mol Pharmacol. 2007; 72:604–611. [PubMed: 17578897]

Patana AS, Kurkela M, Finel M, Goldman A. Mutation analysis in UGT1A9 suggests a relationship between substrate and catalytic residues in UDP-glucuronosyltransferases. Protein Eng Des Sel. 2008; 21:537–543. [PubMed: 18502788]

Rost B, Yachdav G, Liu J. The PredictProtein server. Nucleic Acids Res. 2004; 32(Web Server issue):W321–W326. [PubMed: 15215403]

Soars MG, Ring BJ, Wrighton SA. The effect of incubation conditions on the enzyme kinetics of udp-glucuronosyltransferases. Drug Metab Dispos. 2003; 31:762–767. [PubMed: 12756209]

Starlard-Davenport A, Xiong Y, Bratton S, Gallus-Zawada A, Finel M, Radominska-Pandya A. Phenylalanine(90) and phenylalanine(93) are crucial amino acids within the estrogen binding site of the human UDP-glucuronosyltransferase 1A10. Steroids. 2007; 72:85–94. [PubMed: 17174996]

Stewart JJ. Optimization of parameters for semiempirical methods V: modification of NDDO approximations and application to 70 elements. J Mol Model. 2007; 13:1173–1213. [PubMed: 17828561]

Wells PG, Mackenzie PI, Chowdhury JR, Guillemette C, Gregory PA, Ishii Y, Hansen AJ, Kessler FK, Kim PM, Chowdhury NR, Ritter JK. Glucuronidation and the UDP-. 2004

Xiong Y, Bernardi D, Bratton S, Ward MD, Battaglia E, Finel M, Drake RR, Radominska-Pandya A. Phenylalanine 90 and 93 are localized within the phenol binding site of human UDP-

glucuronosyltransferase 1A10 as determined by photoaffinity labeling, mass spectrometry, and site-directed mutagenesis. Biochemistry. 2006; 45:2322–2332. [PubMed: 16475821]

Zhang H, Tolonen A, Rousu T, Hirvonen J, Finel M. Effects of Cell Differentiation and Assay Conditions on the UDP-glucuronosyltransferases Activity in Caco-2 Cells. Drug Metab Dispos. 2011; 39:456–464. [PubMed: 21098645]

Zielinska A, Lichti CF, Bratton S, Mitchell NC, Gallus-Zawada A, Le VH, Finel M, Miller GP, Radominska-Pandya A, Moran JH. Glucuronidation of monohydroxylated warfarin metabolites by human liver microsomes and human recombinant UDP-glucuronosyltransferases. J Pharmacol Exp Ther. 2008; 324:139–148. [PubMed: 17921187]

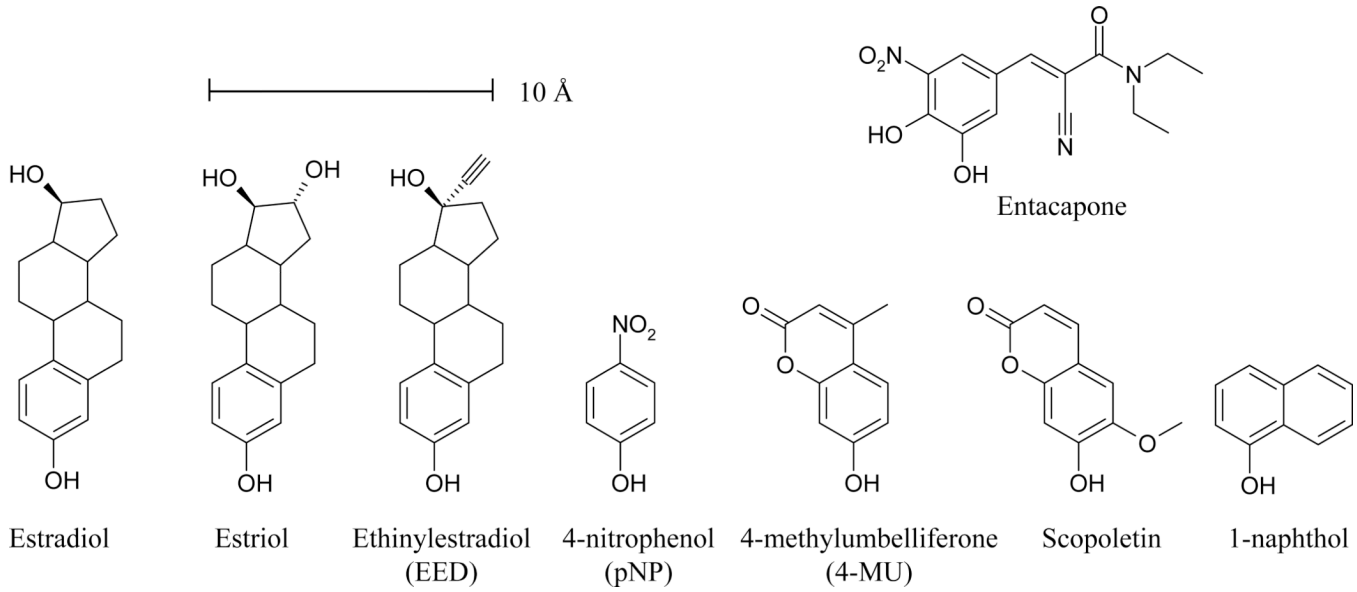

Fig. 1.
Molecular structures of the eight substrates used in the screening assays. The compounds are oriented so that the reactive hydroxyls point down.

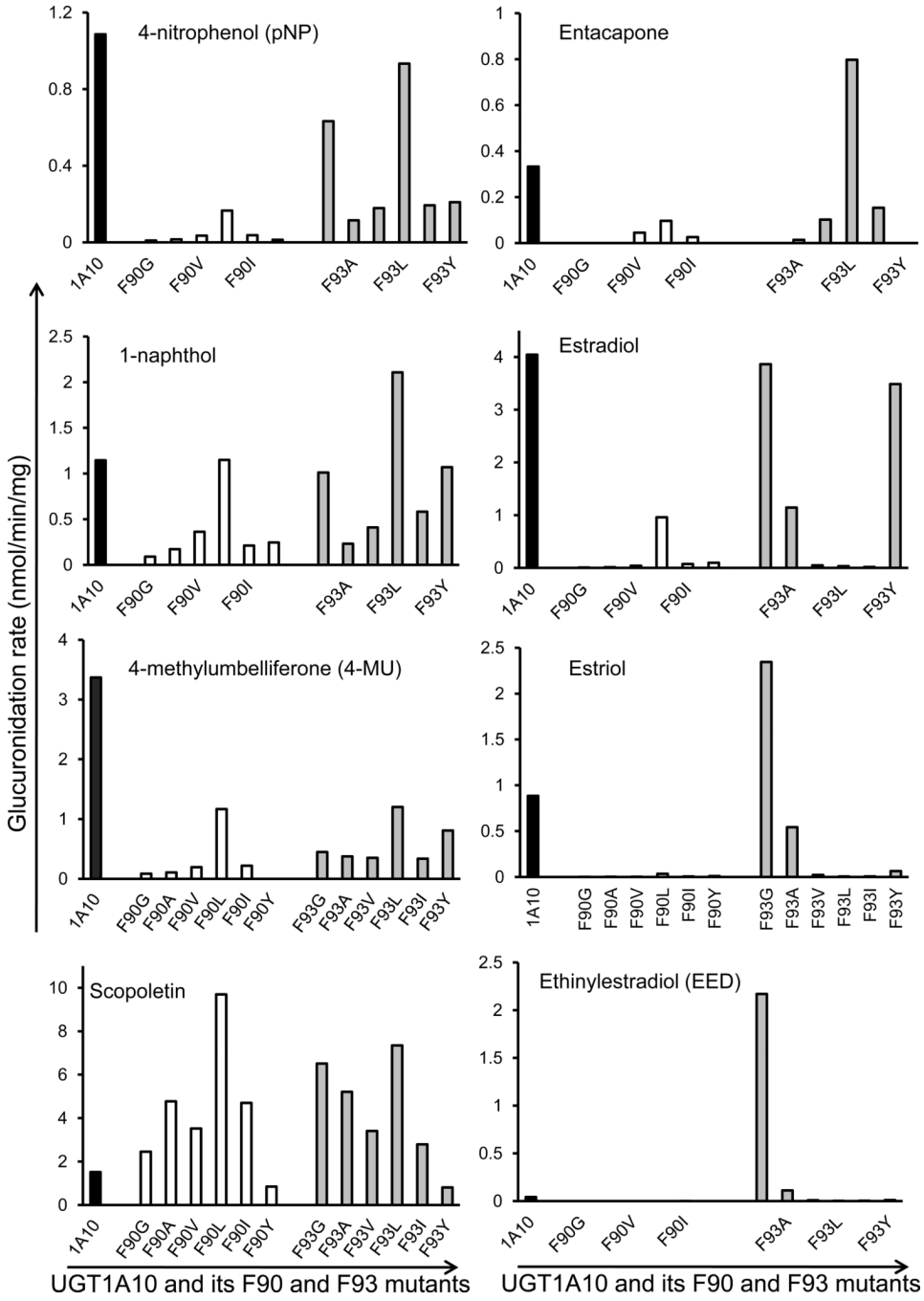

Fig. 2.

Glucuronidation rates of the 8 substrates by UGT1A10 and the 12 mutants. These screening assays were carried out at a single substrate concentration, as follow: scopoletin, pNP, entacapone and estriol, 500 μM; 4-MU, 200 μM; estradiol, EED and 1-naphthol, 100 μM. The rates were corrected (normalized) according to the relative expression levels of the UGT in each preparation (see Methods). The units for all the Y axes are nmol/min/mg (see arrow on the left side) and the mutants are indicated on the X-axes (see arrows at the bottom).

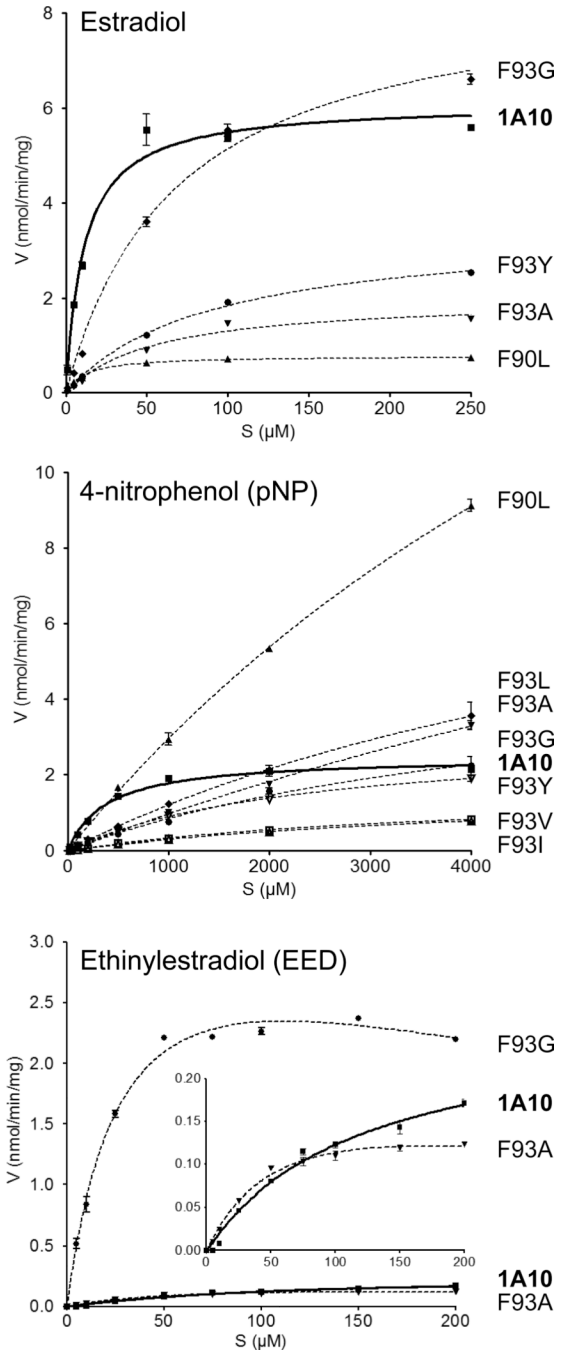

Fig. 3.

Kinetic analyses of estradiol (3-OH), 4-nitrophenol (pNP) and ethinylestradiol (EED) glucuronidation by UGT1A10 and the mutants that exhibited considerable activity toward the respective substrate (Fig. 2). The rates were corrected for relative expression levels and the derived kinetic constants are listed in Table 1.

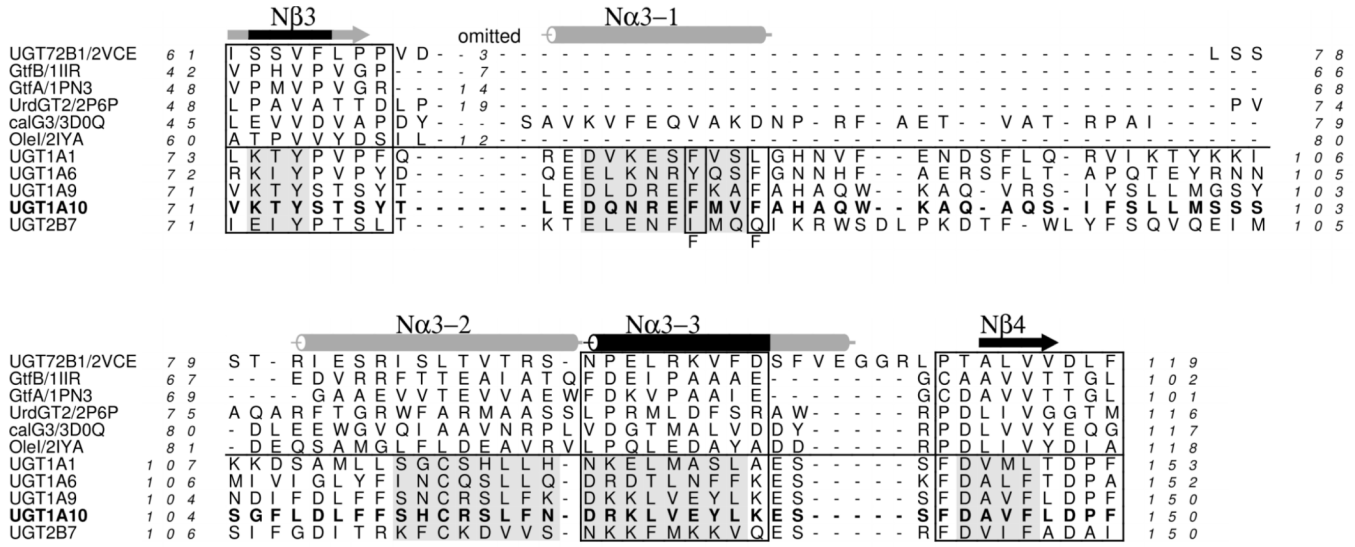

Fig. 4.

Sequence to structure alignment between structurally-solved glycosyltransferases (6 upper sequences) and selected human UGTs. The secondary structure elements of the crystal structures of the glycosyltransferases are shown above the sequences; those present in all proteins are colored black, and those found in some but not all crystals are gray. The boxed areas mark segments that are fully super-imposable among all structures. The predicted helices and strands of the UGT sequences are indicated with gray background. UGT1A10 sequence is in boldface and its F90 and F93 are marked below the sequences. Numbers indicate residues before and after the shown fragments (including the signal sequences, in case of the UGTs), or the number of residues omitted from five protein structures before Nα3-1. The enzymes with known crystal structures, and the structure codes, are: UGT72B1/2VCE, the hydroquinone glucosyltransferase from *Arabidopsis thaliana*; GtfB/1iir, the TDP-epi-vancosaminyltransferase GtfB from *Amycolatopsis orientalis*; GtfA/1PN3, GtfA from the latter organism; UrdGT2/2P6P, the C-C bond-forming DTDP-D-olivose-transferase from *Streptomyces fradiae*; calG3/3d0q, the enediyne glycosyltransferase from *Micromonos poraechinospora*; OleiI/2iya, the oleandomycin glycosyltransferase from *Streptomyces antibioticus*.

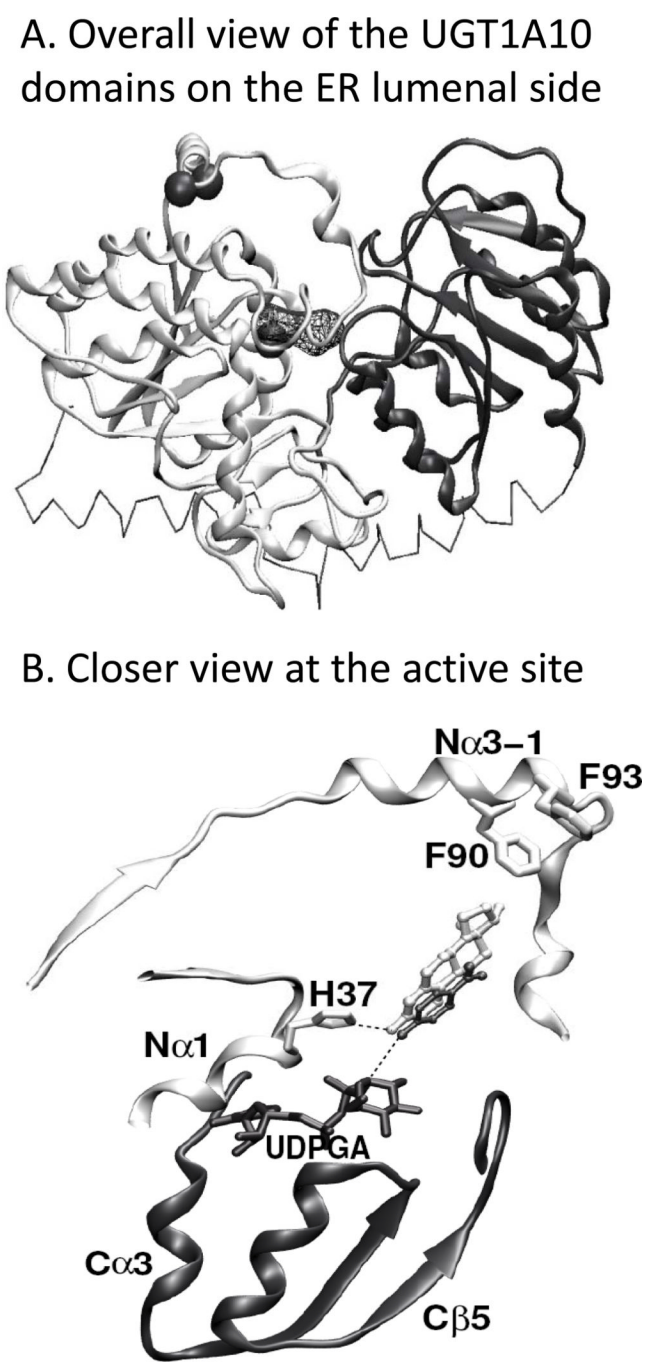

Fig. 5.

A structural model of UGT1A10. A. An overall view of the lumenal part of the enzyme. The N-terminal domain is shown in white cartoon representation, the C-terminal domain is in dark grey cartoon, and the envelop helices are shown as a black Ca-trace (see Laakkonen and Finel (2010) for a details description of the domains in a UGT enzyme). The spheres represent the locations of F90, F93 and the “catalytic His”, H37. The location of the reactive site is marked with a space-filling mesh. The endoplasmic reticulum membrane is just underneath the shown model. B. A close-up view of the active site of the enzyme. The N-terminal domain (in white) is up, and the C-terminal domain (in dark gray) is down. Residues discussed in this study, as well as the structural elements they interact with, are

shown and named. Estradiol and 4-nitrophenol (pNP) were docked to putative reactive distance and orientation with respect to His 37 and the bound UDPGA. Estradiol is shown in white ball-and-stick representation, and pNP in dark gray.

Table 1

Kinetic parameters for 4-nitrophenol (pNP), estradiol (at the 3-OH) and ethinylestradiol (EED) glucuronidation by UGT1A10 and the mutants. Empty boxes indicate that kinetic analyses were not done due to very low, if any, detectable activity. The V_{max} values were corrected for relative expression level (see Methods).

UGT	4-nitrophenol (pNP)				Estradiol				Ethinylestradiol (EED)			
	K_m* (μM)	V_{max} (nmol/min/mg)	K_{cat} (V_{max}/K_m)	Goodness of fit (R^2)	K_m (μM)	V_{max} (nmol/min/mg)	K_{cat} (V_{max}/K_m)	Goodness of fit (R^2)	K_m (μM)	V_{max} (nmol/min/mg)	K_{cat} (V_{max}/K_m)	Goodness of fit (R^2)
1A10	386.9 ± 73.5	2.46 ± 0.14	6.36×10^{-6}	0.93	11.06 ± 1.37	6.10 ± 0.17	5.5×10^{-4}	0.97	122.5 ± 18.0	0.27± 0.02	2.20×10^{-6}	0.98
F90A												
F90L	12331 ± 1916	38.3 ± 4.5	3.11×10^{-6}	0.99	12.1 ± 1.7	0.78 ± 0.03	6.45×10^{-5}	0.96				
F90G												
F90V												
F90I												
F90Y												
F93A	16210 ± 4780	16.6 ± 4.1	1.02×10^{-6}	0.99	54.0 ± 9.5	1.99 ± 0.12	3.69×10^{-5}	0.92	65.7 ± 16.4 K_i (μM) 454 ± 231	0.21 ± 0.03	3.20×10^{-6}	0.99 (substrate inhibition)
F93L	7418 ± 2344	10.2 ± 2.3	1.38×10^{-6}	0.97								
F93G	5203 ± 870	5.23 ± 0.6	1.01×10^{-6}	0.99	67.6 ± 7.3	8.63 ± 0.35	1.28×10^{-4}	0.99	30.9 ± 3.6 K_i(μM) 401 ± 86	3.66 ± 0.2	1.18×10^{-4}	0.99 (substrate inhibition)
F93V	4064 ± 408	1.65 ± 0.10	0.41×10^{-6}	0.99								
F93I	5021 ± 308	1.74 ± 0.07	0.35×10^{-6}	0.99								
F93Y	2383 ± 121	3.03 ± 0.08	1.27×10^{-6}	0.99	89.0 ± 4.9	3.49 ± 0.08	3.92×10^{-5}	0.99				

*The K_m values for the mutants, as well as the K_i values in the cases of observed substrate inhibition kinetics, were determined by extrapolation since they were outside the (broad) tested concentration range.